Comparison of High-Speed PM Machine Topologies for Electrically-Assisted Turbocharger Applications

A. Gilson*, F. Dubas**, D. Depernet** and C. Espanet*
* Research and Development Dept., Moving Magnet Technologies, Besançon, France
** Energy Dept., FEMTO-ST Institute, University of Bourgogne Franche-Comté, Belfort, France

***Abstract*--This paper presents a performance comparison between different high-speed (HS) permanent-magnet (PM) topologies for electrically assisted turbocharger (EAT) applications. The focus of the research is mainly on the efficiency and torque capability comparison of three surface-mounted PM machines: a slotless toroidally wound, and two 6-slot machines having different slot shapes. The base specification of the application is 15 kW @ 150 krpm. Mechanical considerations and general guidelines are also given in the paper to ensure a realistic design of the motor regarding the application. This paper shows that while one topology offers the highest efficiency but a poor torque density, the other two give a better compromise.**

***Index Terms*—Eddy current, finite element analysis, high-speed permanent magnet machines, toroidal machines.**

I. Introduction

High-speed machines (HSM) have become an interesting solution for demanding applications where a little space is available and reduced weight is needed. HSM machines are as a consequence increasingly used in many fields [1 – 3] including electrically assisted turbochargers (EAT). EATs enable turbo-lag reduction, power regeneration and overall efficiency improvement for the vehicle.

However, the choice of the best machine topology is always challenging [4] since it depends on many factors such as: Environment (temperature, volume size and shape, etc.), specifications (torque, speed, acceleration, etc.) and cost. In the field of HSM, PM and switched reluctance machines (SRM) are a popular options, especially in that range of speed and power. For example, considering the factors described above, machine designers tends to use SRMs when cost is critical in the application [5] and PM machines when the torque density becomes the leading factor.

This paper addresses this issue of selecting the best topology for an EAT of 15 kW @ 150 krpm. The study is limited to the comparison of surface PM machines with different kind of stators. The efficiency and torque capability is investigated for each machine and it is found that, in the same volume, one of the machines achieves the best efficiency but has the lowest torque density while the other two are able to offer a good comprise.

In the first part of this paper, the method is detailed with the presentation of the studied topologies, design parameters and calculation procedure using finite element analysis (FEA). In the second part, the results of the study are presented, discussed and some key elements are given to improve the accuracy of the simulations.

II. Method

A. Presentation

The study is carried out using a FEA software (Cedrat Flux2D®). Different PM machine topologies are selected based on the relative simplicity of their manufacturing process (e.g. 3-phase, low number of slots) and the application requirement (2-pole rotor). The proposed topologies are shown in Fig. 1 and consist in: A slotless toroidally wound machine (slotless) because of its large air gap and winding arrangement, a 6-slot machine with straight teeth (slotted 1) for its simple manufacturing process and a 6-slot machine with tooth tips for its torque density (slotted 2).

The next paragraphs of this section present in detail the design rules chosen for the three proposed topologies, the variation parameters used and how the different losses and torque are evaluated.

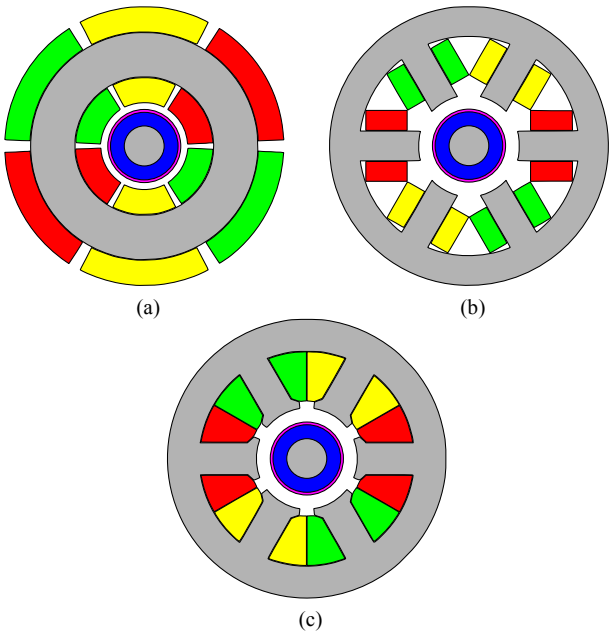

Fig. 1. Proposed high-speed topologies. (a) Slotless toroidally wound (slotless). (b) 6 slots with 6 concentrated coils on straight teeth (slotted 1). (c) 6 semi-closed slots with 6 concentrated coils (slotted 2).

B. Machine Design

The different machines are compared according to a number of design rules described in this section. Thus, the number of parameters that defined both rotor and stator can be reduced. Firstly, the entire machine must be contained in a cylinder of radius R_0 and length L_0. Secondly, materials are selected and are not a part of the parametric study. Their properties are given in the appendix. Finally, the two following subsection describe the specific design choices concerning the rotor and stator.

1) Rotor

Mechanical considerations such as rotor tip speed and critical speeds have to be taken into account to obtain a realistic design of the machine. Since the torque of the machine is proportional to the rotor volume [6] and the length over diameter ratio (1) must be small to prevent rotor instability [7], the rotor diameter is selected by taking the biggest affordable diameter at this level of speed. Consequently, the tip speed v defined by (2) is set to be less than 200 m/s.

$$\lambda = \frac{L_{st}}{2R_{sh}} \tag{1}$$

$$v = (R_{sh} + H_{ma})\omega \tag{2}$$

where L_{st} is both the stack length of the machine and the active part of the rotor, R_{sh} the shaft radius, H_{ma} the magnet thickness and ω the rotational speed. This model neglect the additional rotor length needed to actually build the machine such as bearings and other mechanical elements. The magnet onto the shaft is considered to be an additional mass and does not contribute to the stiffness of the rotor.

The retaining sleeve is calculated to withstand the centrifugal forces and prevent the magnet from scattering. The mechanical considerations to calculate the thickness of the sleeve are detailed in [8] and will not be described in this paper.

Table I summarizes the selected geometrical parameters of the rotor according to the described method. The air gap is defined as the distance between the sleeve and the copper for the toroidal machine and as the distance between the sleeve and the stator bore in the slotted case. Both magnet and air gap thickness are not a part of the parametric study.

TABLE I
ROTOR DIMENSIONS

Parameter	Slotless	Slotted 1	Slotted 2	Unit
Shaft radius (R_{sl})	14			$\%R_0$
Magnet thickness (H_{ma})	10			$\%R_0$
Sleeve thickness (H_{sl})	4			$\%R_0$
Air gap (H_{ag})	3	10	10	$\%R_0$

2) Stator

As described in the introduction of this section, each machine is contained in a given cylinder. The end-windings of the different machines must also be contained in these dimensions and impact the active length. In addition, the following design rules applied:

- For the slotless toroidal topology: The yoke and copper thickness change to keep the outer radius equal to R_0.
- For the three topologies: The yoke thickness impact the end-winding length in order to keep the overall length equal to L_0.
- For the slotted topologies: The stator yoke thickness is always equal to the tooth thickness.
- For the slotted topology with tooth tips: Only two tooth tip opening angle are investigated.

The variation parameters of the three stators are summarized in Table II.

TABLE II
VARIATION PARAMETERS

Parameter	Slotless	Slotted 1	Slotted 2	Unit
Stator yoke/tooth thickness (H_{sy})	8~48	14~26	14~26	$\%R_0$
Tooth tip opening (β)	–	–	45;50	deg
Stack length (L_{st})	Depends on H_{sy}			

C. Machine Torque and Efficiency Evaluation

The losses are calculated for each topology and configuration, they are divided into: copper loss, iron loss in the stator laminations, rotor eddy current loss and mechanical loss (bearings and windage). The impact of AC loss in the winding (skin and proximity effect) is not taken into account in this paper but eddy current loss in the housing (toroidal machine) is briefly investigated at the end of the paper.

The three machines are calculated at a rated power of 15 kW @ 150 000 rpm. In order to produce torque, sinusoidal currents are applied in phase with the fundamental component of the machine back-EMFs. Since the current amplitude to reach the required torque is unknown when running the first simulation, it is necessary to run at least two simulations to converge towards the operating point.

For each machine and configuration, efficiency and torque capability is evaluated. A diagram of the different losses and where they occur is depicted in Fig. 2. In addition, the comparison between the three machine topologies is conducted at the temperature of 110°C. The temperature impact the winding resistance and magnet remanence as described by (3) and (4).

$$Br(T) = Br_0[1 + \alpha_{Br}(T - T_0)] \tag{3}$$

where Br_0 is the magnet remanent flux density at T_0 and α_{Br} the temperature coefficient. In the same way, the electrical resistivity of the copper winding is defined for any temperature by the following equation:

$$\rho_{Cu}(T) = \rho_{Cu,0}[1 + \alpha_{Cu}(T - T_0)] \tag{4}$$

where $\rho_{Cu,0}$ is the electrical resistivity of copper at T_0 and α_{Cu} the temperature coefficient.

The following paragraphs describe the different losses occurring in the machines to compute the efficiency. The motor constant is also introduced to evaluate the torque density of the machine.

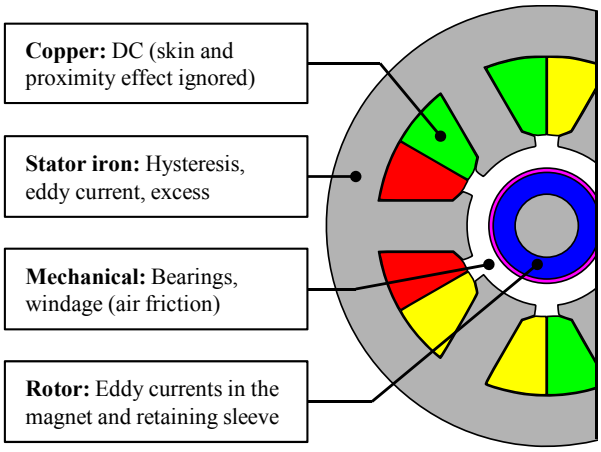

Fig. 2. Overview of slotted 2 with a short description of the losses and where they occur.

1) Copper

The copper losses are simply defined as follow:

$$P_{cu} = 3RI_{rms}^2 \tag{5}$$

where I_{rms} is the rms value of the phase current and R the phase resistance. The AC components of the copper loss such as skin and proximity effects are ignored in this study.

2) Stator Iron

These losses are calculated using the Bertotti module available in the FEA software. It is based on the following equation:

$$P_{Fe} = m_{Fe} \cdot \left(k_{hy} f B^2 + k_{ec} f^2 B^2 + k_{ex} f^{3/2} B^{3/2}\right) \tag{6}$$

where m_{Fe} is the stator mass, k_{hy}, k_{ec} and k_{ex} are respectively the hysteresis, eddy current and excess loss coefficients, f the fundamental frequency and B the peak value of the flux density. This equation assumes a sinusoidal time varying flux density.

3) Rotor Eddy Current

The rotor eddy current loss is directly calculated by the FEA software using a transient simulation. The accuracy of the results is ensured by using 3 mesh elements in a skin depth of the material and an appropriate time step.

4) Mechanical

They are divided into bearing losses and windage loss. First, the bearing losses depend on the technological choice (ball bearings, foil, magnetic, etc.). Since they do not impact the results of this study, an arbitrary value of 100 W is selected. Second, windage loss is caused by air friction in the air gap and is calculated thanks to the following equations described in [9]:

$$P_{win} = \pi C_d \rho_{air} (R_{sh} + H_{ma} + H_{sl})^4 \omega^3 L_{st} \tag{7}$$

where C_d is the skin friction coefficient, ρ_{air} is the density of the air taken equal to 1.09 kg/m^3, L_{st} the length of the active part of the rotor. C_d is defined as:

$$\frac{1}{\sqrt{C_d}} = 2.04 + 1.768 \cdot ln\left(Re\sqrt{C_d}\right) \tag{8}$$

where Re is the Reynolds number.

5) Motor constant

The torque density of the machine is reflected in the motor constant coefficient Km, which is defined by:

$$Km = \frac{T_{mag}}{\sqrt{P_{Cu}}} \tag{9}$$

where T_{mag} is the torque produced by the machine.

III. Results

A. Description

The final designs provide a 94.8 to 96.5% motor efficiency and a motor constant between 58.1 and 79.6 mNm/$\sqrt{\text{W}}$. As show in Fig. 3, the toroidal topology is the only one to almost provide an optimum in both efficiency and motor constant with the same configuration ($H_{sy} = 28\sim32\ \%R_0$). Figure 4 shows that for the slotted machine with straight teeth, the maximum efficiency is reached at $H_{sy} = 23\ \%R_0$ whereas the motor constant is the highest for $H_{sy} = 14\ \%R_0$. The same phenomenon occurs for the slotted machine with tooth tips (Fig. 5) and shows that a compromise between efficiency and torque density has to be found for both slotted topologies.

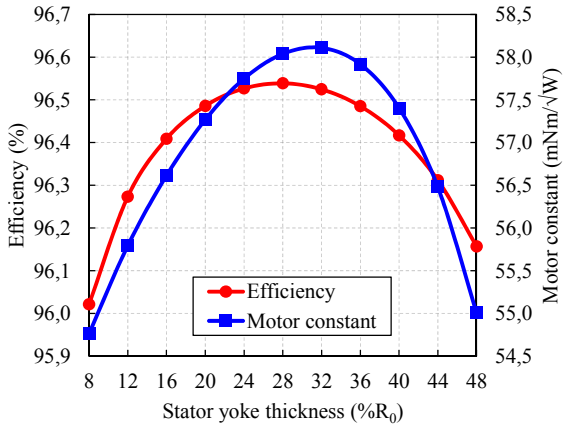

Fig. 3. Efficiency and motor constant for the toroidal machine.

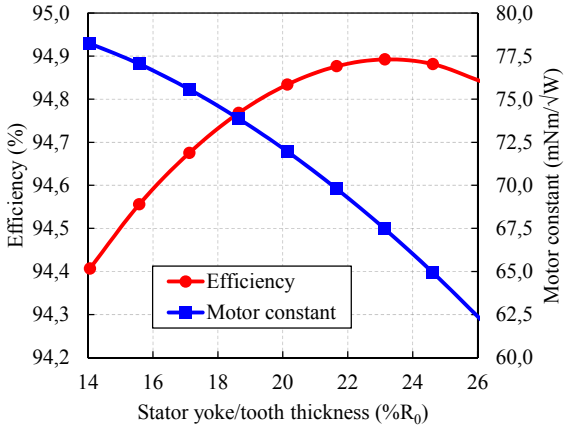

Fig. 4. Efficiency and motor constant for the slotted machine 1 (straight teeth).

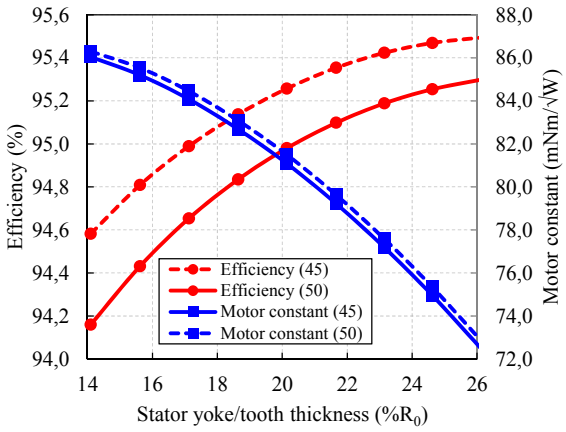

Fig. 5. Efficiency and motor constant for the slotted machine 2 (tooth tip). In the caption, the value between brackets is the tooth tip angle β.

In order to study the losses distribution, a set of machines has been selected among the most efficient ones and their characteristics are displayed in Table III. The losses distribution presented in Fig. 6 shows that mostly copper losses occur in the slotless machine when iron losses are the most significant in the slotted topologies.

TABLE III
SELECTED DESIGNS

Parameter	Slotless	Slotted 1	Slotted 2	Unit
Yoke/teeth thickness (H_{sy})	32	23	22	$\%R_0$
Stack length (L_{st})	76.9	82.5	65	$\%L_0$
Tooth tip opening (β)	–	–	45	deg
Motor constant (Km)	58.1	67.5	79.6	mNm/$\sqrt{W}$
Efficiency (η)	96.5	94.9	95.4	%

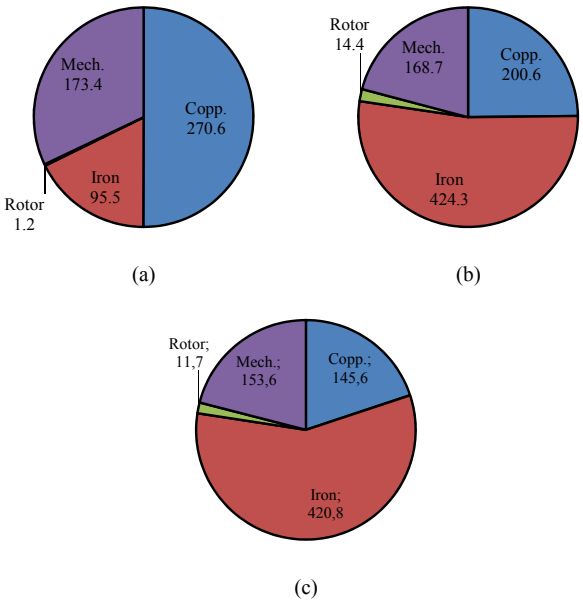

Fig. 6. Loss distribution in the selected designs. (a) Slotless toroidally wound. (b) 6 slots with 6 concentrated coils on straight teeth. (c) 6 semi-closed slots with 6 concentrated coils.

B. Discussion

Although the rotating speed is as high as 150 000 rpm, rotor losses are reasonably low for each topology (between 1 and 15 W as shown in Fig. 7). The main reasons are: The air gap is large enough to filter high order harmonics in the case of the slotted topologies and the current waveform is perfectly sinusoidal. In addition, a non-conductive sleeve has been chosen to retain the magnets.

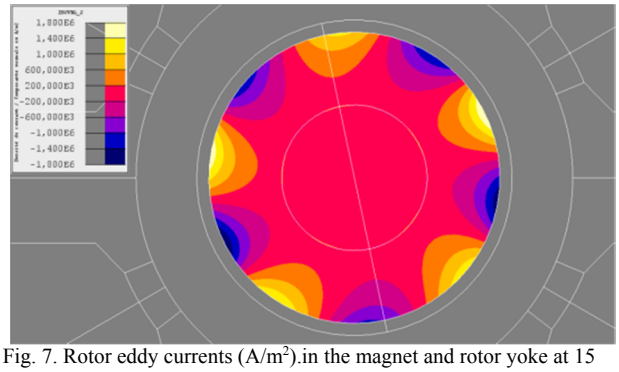

Fig. 7. Rotor eddy currents (A/m^2).in the magnet and rotor yoke at 15 kW and 150 krpm for the selected semi-closed slots stator topology and a non-conductive sleeve.

When integrating these machines into a conductive housing, the toroidal machine will have additional losses due to the eddy current induced by the outside part of the coils. These losses were not included in the comparison presented in this paper and would lead to additional losses.

The slotted machine 2 is much shorter than the other two and would be the best choice in terms of rotor dynamic.

IV. Conclusion

In this paper, the efficiency and torque density of three PM machines topologies dedicated to a 15 kW @ 150 000 rpm EAT have been investigated. The design parameters were described for each structure and a parametric FEA was conducted to calculate the different configurations. The main results of this work are:

- The slotless topology is the most efficient and it is possible to find a configuration leading to both high efficiency and high torque density.
- Even though the slotted topologies are less efficient, the difference is below 1.6% and their torque density is much higher.
- From a mechanical point of view, the structure with the shortest rotor is the best choice. In this study, it is the slotted machine with tooth tips.

There are several important aspects not addressed in this paper that could be investigated for future works:

- Current harmonics: The armature current was assumed sinusoidal. Adding time harmonics could lead to increased rotor losses.
- Thermal: Since the three topologies are geometrically different, the thermal behavior is also different meaning that the motor constant coefficient is not enough to describe accurately the torque density. A thermal model of each machine has to be made to address this issue.

APPENDIX

TABLE IV
SINTERED NDFEB MAGNET PROPERTIES @ T_0=25°C

Parameter	Value	Unit
Remanent flux density (Br_0)	1.19	T
Electrical resistivity (ρ_{ma})	1.5	μΩm
Br temp. coefficient (α_{Br})	-0.10	%/°C

TABLE V
COPPER WINDING PROPERTIES @ T_0=25°C

Parameter	Value	Unit
Electrical resistivity ($\rho_{Cu,0}$)	1.72×10^{-2}	μΩm
ρ temp. coefficient (α_{Cu})	0.39	%/°C

TABLE VI
NO20 STATOR LAMINATION STEEL PROPERTIES

Parameter	Value	Unit
Sheet thickness (d)	0.2	mm
Electrical resistivity (ρ_{Fe})	0.52	μΩm
Density ($\rho_{m,Fe}$)	7650	kg/m^3
Hysteresis coefficient (K_{hy})	1.72×10^{-2}	W/kg s/T^2
Eddy current coefficient (K_{ec})	1.65×10^{-5}	W/kg (s/T)^2
Excess coefficient (K_{ex})	2.50×10^{-4}	W/kg (s/T)$^{1.5}$

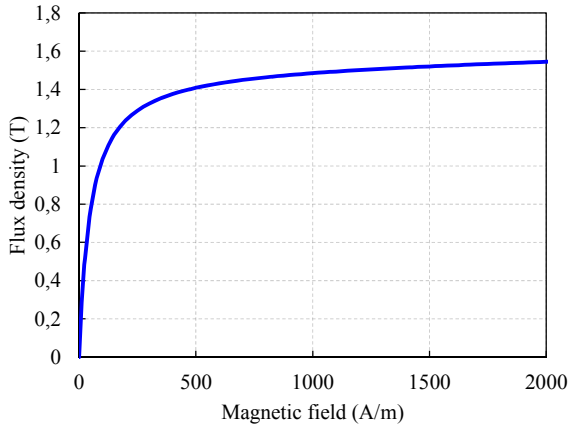

Fig. 8. B(H) curve for the NO20 lamination steel.

REFERENCES

[1] A. Tenconi, S. Vaschetto, and A. Vigliani, "Electrical Machines for High-Speed Applications: Design Considerations and Tradeoffs," *IEEE Transactions on Industrial Electronics*, vol. 61, no. 6, pp. 3022–3029, Jun. 2014.

[2] D. K. Hong, B. C. Woo, J. Y. Lee, and D. H. Koo, "Ultra High Speed Motor Supported by Air Foil Bearings for Air Blower Cooling Fuel Cells," *IEEE Transactions on Magnetics*, vol. 48, no. 2, pp. 871–874, Feb. 2012.

[3] D. Lusignani, D. Barater, G. Franceschini, G. Buticchi, M. Galea, and C. Gerada, "A high-speed electric drive for the more electric engine," in *Energy Conversion Congress and Exposition (ECCE)*, 2015, pp. 4004–4011.

[4] D. Gerada, D. Borg-Bartolo, A. Mebarki, C. Micallef, N. L. Brown, and C. Gerada, "Electrical machines for high speed applications with a wide constant-power region requirement," in *International Conference on Electrical Machines and Systems (ICEMS)*, 2011, pp. 1–6.

[5] S. Kachapornkul, P. Somsiri, R. Pupadubsin, N. Nulek, and N. Chayopitak, "Low cost high speed switched reluctance motor drive for supercharger applications," in *15th International Conference on Electrical Machines and Systems (ICEMS)*, 2012, pp. 1–6.

[6] B. Riemer, M. Leßmann, and K. Hameyer, "Rotor design of a high-speed Permanent Magnet Synchronous Machine rating 100,000 rpm at 10kW," in *2010 IEEE Energy Conversion Congress and Exposition*, 2010, pp. 3978–3985.

[7] A. Borisavljevic, *Limits, Modeling and Design of High-Speed Permanent Magnet Machines*, 2013 edition. Berlin; New York: Springer, 2012.

[8] P.-D. Pfister and Y. Perriard, "Very-high-speed slotless permanent-magnet motors: Analytical modeling, optimization, design, and torque measurement methods," *IEEE Transactions on Industrial Electronics*, vol. 57, no. 1, pp. 296–303, 2010.

[9] J. E. Vrancik, "Prediction of windage power loss in alternators," Oct. 1968.